9084 *Macromolecules* **2007,** *40,* 9084−9093

Codendronized Polymers: Wormlike Molecular Objects with a Segmented Structure

Xingquan Xiong and Yongming Chen*

State Key Laboratory of Polymer Physics and Chemistry, Joint Laboratory of Polymer Sciences and Materials, Institute of Chemistry, The Chinese Academy of Sciences, Beijing 100080, China

Shu Feng and Wei Wang*

The Key Laboratory of Functional Polymer Materials and Institute of Polymer Chemistry, College of Chemistry, Nankai University, Tianjin 300071, China

Received July 8, 2007; Revised Manuscript Received September 12, 2007

ABSTRACT: Herein, we report a series of novel codendronized polymers with an alternating segmented structure prepared by direct radical copolymerization of maleimide pendent with polyester dendron and styrene pendent with Percec-type polyether dendron. These dendronized polymers bearing different dendrons with rather high molar masses as determined by GPC with light scattering detectors were obtained under mild conditions. These novel polymers have been also characterized by ^{1}H NMR, ^{13}C NMR spectroscopy, atomic force microscopy (AFM), and small-angle X-ray scattering (SAXS). All of the codendronized polymers were confirmed to hold an alternating structure; therefore, they have a segmented structure. The SAXS results indicate that these polymers pack hexagonally in bulk, and the materials with self-organized structures-in-structures have been thus obtained whose properties can be tuned by dendron generation. Through further modification of one pendent dendron, amphiphilic codendronized polymers were produced. These dendronized polymers with a segmented structure of different polarity may have a potential to segregate lengthwise, and, therefore, many fascinating properties related to self-assembly are expected.

Introduction

Dendrimers[1] are a class of macromolecules with regular branches and three-dimensional architecture. Normally they are composed of several dendritic wedges (dendrons) linked to a core. Because the size, the number of end groups, and the functionality are tailor-made, their properties can be tuned precisely. Therefore, they have attracted great attention from researchers in chemistry, materials, medicine, and biology in the last two decades.[2]

One important application of dendrimers is to use well-defined dendrons as the building blocks to generate so-called dendronized polymers whose linear backbones bear dendritic wedges at each repeating unit.[3] The most fascinating property of dendronized polymers is that, with increase of dendron generation, they are prone to adopting a wormlike morphology, which is caused by steric repulsion between the grafted bulky groups. Different from conventional polymers, the diameter of dendronized polymers is in order of a few nanometers, and the persistent length is rather long. Their diameter and rigidity can be well controlled by altering dendron generation. Some wormlike polymers have been imaged by scanning force microscopy (SFM), and their conformation can be manipulated by SFM tips.[4] Therefore, dendronized polymers are single molecular nanoobjects, and they have attracted a great attention not only from academia but also from application. Recently, dendronized polymers have emerged as a class of new nanomaterials applied as carriers for drug delivery and supports for homogeneous catalyst, etc.[5]

In general, there are three approaches to synthesize dendronized polymers. The first route is known as the "macromonomer" approach by conducting a chain-growth or step-growth polymerization of dendritic monomers. Its advantage is that each repeated unit bearing a dendron can be guaranteed, and, therefore, the structure is rather uniform. Yet the shortage is that the macromonomers with higher generation often lead to oligomers due to steric obstruction of larger dendrons.[3h,6] The second route is the "graft-onto" route. In this way, perfect dendrons are coupled onto a preformed polymer chain.[7] The last route is the "graft-from" approach, that is, divergent generating dendrons step-by-step from the polymer backbone.[8] Later, two approaches face the problem of incomplete grafting, which leads to a large number of structural defects.

So far, most of the dendronized polymers by the macromonomer approach are prepared by radical homopolymerization; therefore, their structures along the main chains are homogeneous. Some dendronized copolymers are generated by polycondensation, such as Suzuki reaction, of dendritic monomers.[3h,7a,9] However, the polymerization degree by polycondensation is relatively low, and, therefore, formation of the dendronized polymer with a larger ratio of length to diameter is difficult. So far, radical polymerization has been proved to be the most efficient way to generate the long enough dendronized polymers.[10]

To endow the functions to these molecular worms, the radical copolymerization of dendritic monomer and functional monomer or two different dendritic monomers may be a choice. Yet uncontrolled copolymerization and statistic distribution of segments may contravene the intention to tailor the structure of dendronized polymers. Recently, this group has reported the alternating radical copolymerizations of styryl macromonomer bearing Fréchet-type dendrons of different generation and maleic anhydride or maleimide.[11,12] A series of novel dendronized copolymers with rather high molar masses have been obtained under mild conditions; reactive and functional groups have been

---

* Corresponding authors. E-mail: ymchen@iccas.ac.cn. E-mail: weiwang@nankai.edu.cn.

10.1021/ma071507y CCC: $37.00 © 2007 American Chemical Society
Published on Web 11/09/2007

Scheme 1. Structure of Monomers and Strategy To Prepare the Codendronized Polymers 2[G2]6[G2] by Radical Polymerization

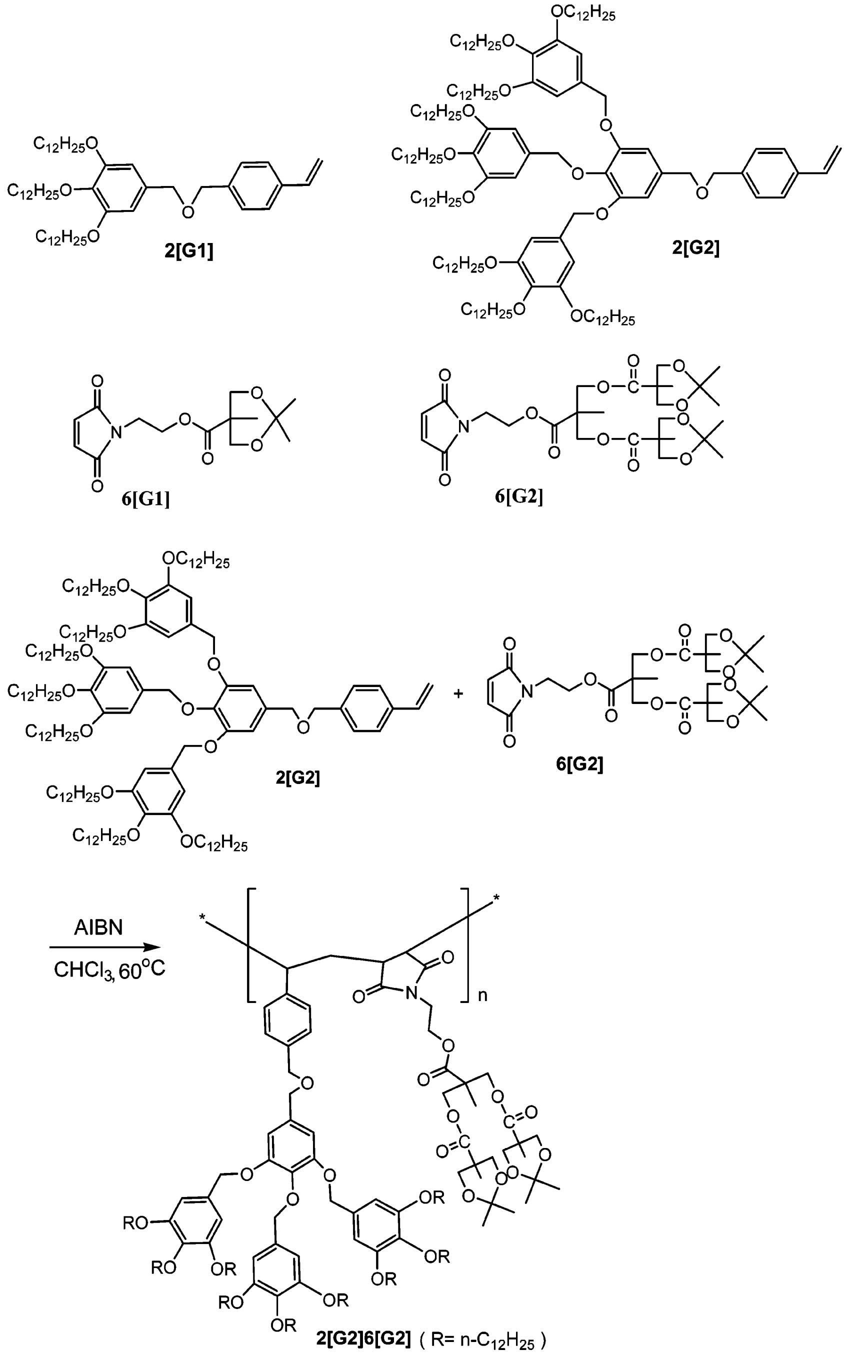

uniformly dispersed along the molecular worms. Radical copolymerization of styryl dendron and maleic anhydride or maleimide still has a strong tendency to form alternating sequence, and, therefore, this is an effective method to functionalize dendronized polymers while the uniformity can be maintained. Furthermore, we have prepared codendronized polymers by a combination of macromonomer and graft-from approach.[13] The copolymerization of styryl dendrimer and *N*-(2-hydroxyethyl)maleimide produced dendronized copolymers, and then the second type of dendron was grafted from the hydroxyl groups via a divergent method. Still, the defects can be produced during introduction of a second dendron due to the crowded branches.

In this Article, we report the radical copolymerization of two dendritic monomers that produces a series of novel codendronized polymers bearing two kinds of pendent dendritic wedges. Because the copolymerizing units, styrene and maleimide, have a strong tendency to give an alternating sequence, two kinds of dendrons are expected to pack alternately, and, therefore, novel segmented polymers with defect-free structure may be prepared. As far as we know, it is the first report on radical copolymerization of two dendritic macromonomers that produced uniform polymer chains. The SAXS characterizations demonstrate that these codendronized polymers in bulk form an ordered structure with a hexagonal packing. Finally, we removed the protecting groups on periphery of one dendron, and amphiphilic codendronized polymers were obtained.

Results and Discussion

It is known that radical copolymerization of styrene and maleic anhydride or maleimide generates the copolymers with a strict alternating sequence. Previously, we have demon-

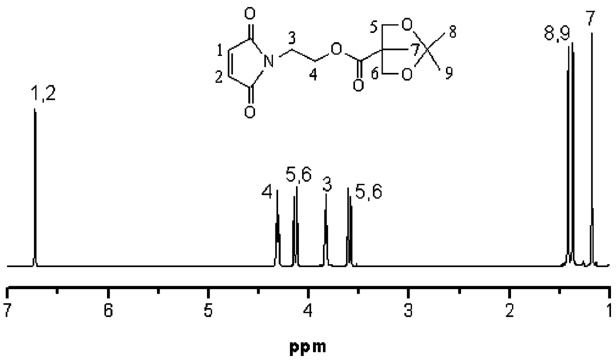

Figure 1. ^{1}H NMR spectrum of **6[G1]** monomer in $CDCl_3$ with assignment.

Scheme 2. Synthesis of Styryl Dendrimers 2[G1, G2]

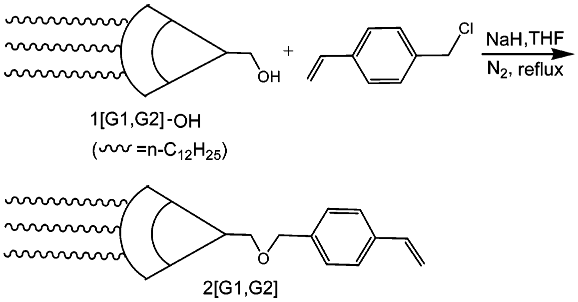

strated that the bulky styryl dendritic monomer did not alter copolymerization chemistry.[11−13] Therefore, to get a perfect copolymer with a uniform segmented structure and higher molar mass, we applied the "macromonomer" approach by radical copolymerization of styryl monomer carrying Percec-type polyether dendrons **2[G*n*]** (n = 1, 2) and maleimide monomer bearing polyester dendron **6[G*n*]** (n = 1, 2). Each type of macromonomer carries the dendrons of first and second generation respectively. Therefore, four codendronized polymers can be prepared by crosswise copolymerization of each monomer respectively. Isopropylidene protected maleimide monomer **6[G*n*]** was used for copolymerization, and the protection can be removed afterward to derivate further research on self-assembly. The structure of four monomers and the copolymerization of higher generation monomers are shown in Scheme 1.

Synthesis of Styryl Polyether Dendron 2[G1, G2] and Maleimide Polyester Dendron 6[G1, G2]. As outlined in Scheme 2, the macromonomers **2[G1, G2]** were synthesized by an etherification of Percec-type **1[G1, G2]-OH** with an excess of 4-vinylbenzyl chloride in the presence of NaH in THF. The structures of **2[G1, G2]** were conformed by ^{1}H NMR, ^{13}C NMR spectroscopy, elemental analysis, and MALDI-TOF mass spectrometry, respectively. A detailed procedure of the preparation and the characterization data can be found in the Supporting Information. In the ^{1}H NMR spectra of **2[G1]** and **2[G2]** (Figures S1 and S4 in the Supporting Information), the quadruple peaks at 6.70 ppm stand for the proton of $-CH{=}CH_2$. The double peaks at 5.75 and 5.24 ppm having coupling constants of 17.6 and 10.9 Hz, respectively, are assigned to the *cis*- and *trans*-protons of $-CH{=}CH_2$. There are no obvious chemical shifts of vinyl protons with increase of generations. The carbon signals of the C=C group styrene are recognized at 113 and 136 ppm in the ^{13}C NMR spectra of **2[G1]** and **2[G2]** (Figures S2 and S5). The MALDI-TOF mass spectra of **2[G1]** and **2[G2]** are shown in Figure S3 and Figure S6.

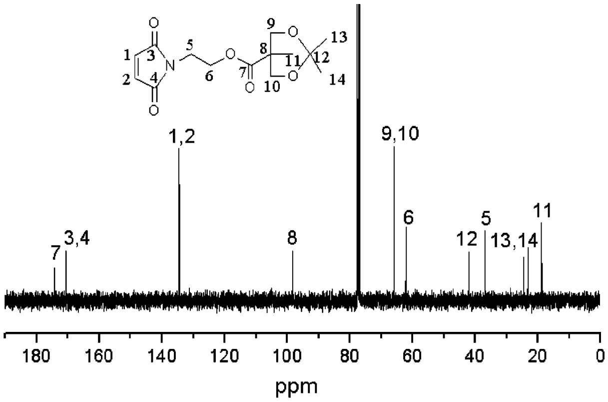

Figure 2. ^{13}C NMR spectrum of **6[G1]** monomer in $CDCl_3$ with assignment.

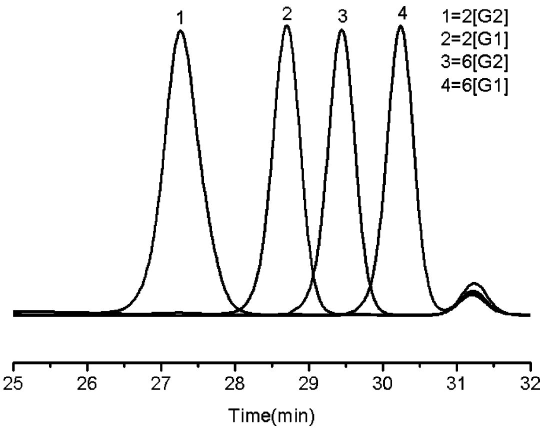

Figure 3. SEC traces of two kinds of dendritic monomers, **2[G1, G2]** and **6[G1, G2]**.

Maleimide monomers **6[G1, G2]** were prepared by a divergent approach, which may generate polyester dendrons as depicted in Scheme 3. At first, when *N*-hydroxylethyl maleimide **3a** reacted with the anhydride monomer **4**, the final products were very complex. The possible reason was the unsaturated C=C bond could react with the organic acid, which was the byproduct during the esterification reaction. So, we applied the furan protected *N*-hydroxylethyl maleimide **3b** to replace **3a**. From the protected maleimide derivative **3b**, the product **5** was synthesized in 85% yield via a 4-dimethylamino pyridine (DMAP)-catalyzed esterification with the anhydride monomer **4**. The imide **5** was deprotected to yield diol **7**, which was further reacted with **4** to generate the dendron **8** of next generation. Deprotection of **5** and **8** by refluxing in toluene at 110 °C for 12 h produced two maleimide monomers **6[G1, G2]** bearing dendritic wedges. The ^{1}H NMR spectrum of **6[G1]** is shown in Figure 1 (see Figure S7 in the Supporting Information for the spectrum of **6[G2]**).

In the ^{1}H NMR spectra of **6[G1]** and **6[G2]**, the two single peaks at 6.72 and 6.73 ppm are assigned to the protons of $CH{=}CH$, respectively. The triple peaks at 4.31 and 3.82 ppm having coupling constants of 5.0 and 5.1 Hz, respectively, are assigned to the protons of H-4 and H-3 of ethylene. The double peaks at 4.13 and 5.59 ppm stand for the resonances of H-5 and H-6. There are three single peaks in higher field, which are assigned to H-8, H-9 of methylene and H-7 of methyl. The carbon signals of the C=C group are recognized in the ^{13}C NMR spectrum at 134.22 ppm (for **6[G1]**) and 134.25 ppm (for **6[G2]**). The other carbon signals can be assigned to the corresponding carbons of

Scheme 3. Strategy To Synthesize Maleimide Dendrimers 6[G1, G2][a]

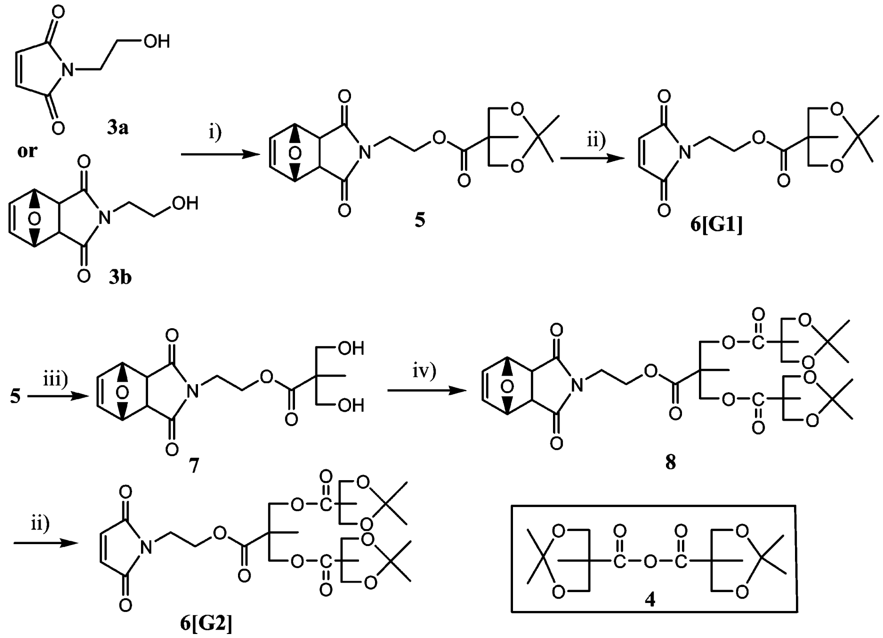

[a] Reagents and conditions: (i) **4**, DMAP, pyridine, CH_2Cl_2, 25 °C, 12 h, 85%; (ii) toluene, reflux, 12 h, 95% for **6[G1]** and **6[G2]**; (iii) Dowex, H^+ resin, MeOH, 3 h, 95%; (iv) **4**, DMAP, pyridine, CH_2Cl_2, 25 °C, 12 h, 60%.

Table 1. Characterization of Four Dendritic Monomers, 2[G1, G2] and 6[G1, G2]

			elemental analysis		SEC data	
monomer	molar mass[a]	$[M + Na^+]^+$ [b]	anal. calcd	found	M_n	M_w/M_n
2[G1]	776.67	799.7	C, 80.35; H, 11.41	C, 80.68; H, 11.28	3250	1.01
2[G2]	2199.89	2222.6	C, 79.11; H, 11.45	C, 78.96; H, 11.36	6800	1.02
6[G1]	297.12	298.0[c]	C, 56.56; H, 6.44; N, 4.71	C, 56.81; H, 6.47; N, 4.85	1480	1.01
6[G2]	569.25	592.1	C, 56.93; H, 6.90; N, 2.46	C, 56.80; H, 6.84; N, 2.57	2180	1.01

[a] Calculated according to the atom weight. [b] Determined by MALDI-TOF mass spectrometry. [c] $[M + H^+]^+$, determined by EI mass spectrometry.

the dendron as shown in Figure 2 (see Figure S8 in the Supporting Information for the spectrum of **6[G2]**).

Size exclusion chromatography (SEC) was applied to characterize the purities of monomers **2[G1, G2]** and **6[G1, G2]**. As demonstrated in Figure 3, the monodispersed peaks were obtained, indicating the coupling reaction and separation were efficient. The actual molar masses were determined by MALDI-TOF mass spectrometry, and the results corresponded to the theoretical values. The detailed information of monomers was collected in Table 1.

Synthesis of the Codendronized Polymers with Alternating Structure through Macromonomer Approach. The copolymerizations of monomers **2[G1, G2]** and **6[G1, G2]** were conducted in chloroform initiated by AIBN at 60 °C, and four codendronized polymers were obtained. As listed in Table 2, the yields of copolymerizations were between 50% and 83%. To get the degrees of copolymerizations (DP), absolute molar masses were determined by GPC equipped with two angle light scattering detectors. In this system, the DP_w's were calculated from the M_w determined by static light scattering by taking one pair of dendritic monomers **2[G1]** and **6[G1]**, **2[G1]** and **6[G2]**, **2[G2]** and **6[G1]**, or **2[G2]** and **6[G2]** as one repeating unit. It was found that the DP_w's of copolymers from low generation monomers, such as **2[G1]6[G1]** and **2[G1]6[G2]**, were rather high. However, the DP_w decreased with increase of macromonomer generations. Although DP could be further increased by optimization of condition, it was believed that size hindrance was the main reason of lower DP.

Table 2. Copolymerization Conditions and Results of the Copolymers[a]

polymer	yield (%)	$M_{w(TALLS)}$	DP_w[b]	M_w/M_n	dn/dc (mL/g)
2[G1]6[G1]	83.4	1 323 000	1230	1.87	0.116
2[G1]6[G2]	57.0	1 813 000	1330	2.60	0.096
2[G2]6[G1]	61.0	322 000	130	1.38	0.106
2[G2]6[G2]	51.0	708 000	280	1.30	0.098

[a] Solvent was chloroform, temperature was 60 °C. Molar ratio of **2[Gn]**:**6[Gn]**:AIBN was 50:50:2. Total concentration of two monomers in solvent was 1.0 mol/L. [b] Calculated from the M_w determined by GPC-TALLS taking one pair of dendritic comonomer as one repeating unit.

The ^1H NMR spectra of four copolymers are similar except the ratios of two components are different. Figure 4 shows the spectrum of polymer **2[G1]6[G1]** with assignment (see Figure S10 in the Supporting Information for the spectra of other copolymers). The broadened peaks are observed, and this is typical for dendronized polymers because of their high DP_w's and the stiffness of their main chains. Because of the overlapping

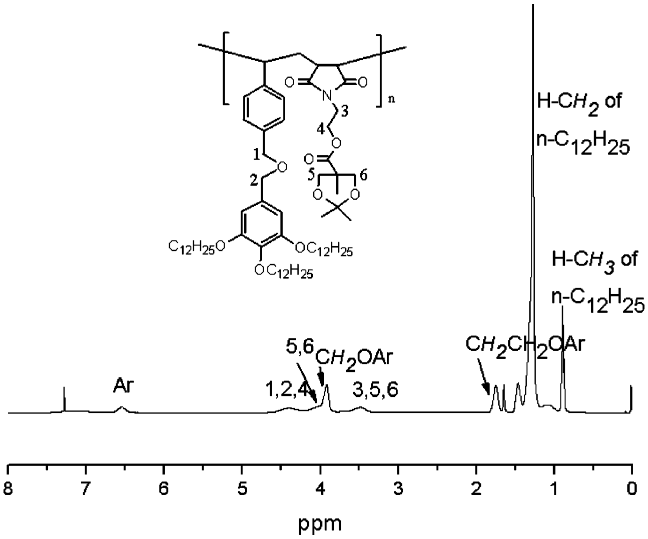

Figure 4. ^{1}H NMR spectrum of polymer **2[G1]6[G1]** in $CDCl_3$ with assignment.

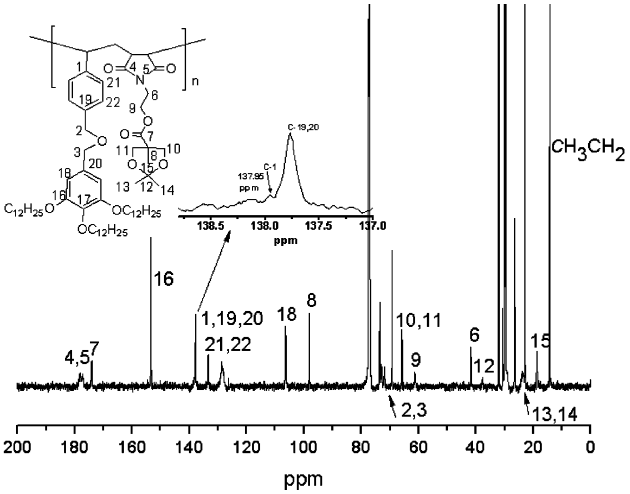

Figure 5. Integrable quantitative carbon NMR spectrum of **2[G1]6-[G1]** in $CDCl_3$ with assignment.

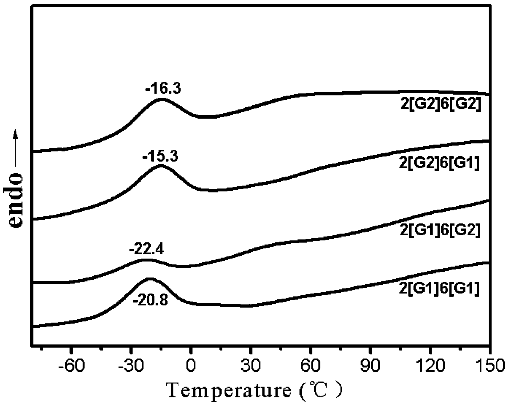

Figure 6. Second DSC heating curves of four codendronized polymers.

of peaks in the ^{1}H NMR spectra, it is difficult to make an accurate estimation of polymer composition by ^{1}H NMR analysis.

According to the literature,[14] we knew that the quaternary carbon of styrene that linked to the polymer chain is very sensitive to the microstructure of copolymers of styrene and maleimide derivatives, and the microstructure could be determined by analyzing the chemical shift of that carbon in ^{13}C NMR spectrum. So we confirmed the alternating sequence structure of polymer **2[G1]6[G1]** and **2[G1]6[G2]** using this method. Previously, we had proven that the position of quaternary aromatic carbon linked to the ether dendron with an alternating structure (C-1 in Figure 5) lies in 138.9−134.9 ppm if the effect of *para*-substituent dendron of styrene was considered.[11,12] Integrable quantitative carbon spectra (Figure 5 for **2[G1]6[G1]**) were obtained by inverse gated-decoupling experiments. The position of C-1 of the copolymer is 137.95 ppm, indicating an alternating sequence. At the same time, the ratio of the integral area of C-2, C-3 from **2[G1]** to C-4, C-5, and C-7 from **6[G1]** is around 1.0 (Figure S11), demonstrating that the ratio of two dendrons in the copolymer is 1:1. Therefore, it was confirmed that the copolymer **2[G1]6[G1]** had a strict alternating sequence in microstructure. The integrable quantitative carbon spectra of **2[G1]6[G2]** (shown in Figures S12 and S13) gave the same conclusion.

In terms of **2[G2]6[G1]** and **2[G2]6[G2]**, their ^{13}C NMR spectra were obtained by increasing their concentration and prolonging the time of ^{13}C NMR experiments. Figure S14 and Figure S15 show the spectra of polymers **2[G2]6[G1]** and **2-[G2]6[G2]** with assignment, respectively. After these spectra were analyzed, the carbon signals of C-1 of these copolymers are recognized in ^{13}C NMR spectra at 138.16 ppm for **2[G2]6-[G1]** and 138.10 ppm for **2[G2]6[G2]**, which lay in 138.9−134.9 ppm. At the same time, their composition could be determined by elemental analysis. The element content of **2-[G2]6[G1]** was determined to be C 76.40 and H 10.75, which accords to the expected composition of 1:1 $(C_{161}H_{275}NO_{19})_n$, C 76.46 and H 10.96. As for **2[G2]6[G2]**, the found and expected values are C 74.34, H 10.42 and C 74.61, H 10.61, respectively, which agreed well. On the basis of the results of ^{13}C NMR spectra and elemental analysis, we can draw a conclusion that these copolymers have strict alternating sequences in microstructure.

Differential Scanning Calorimetry (DSC) Analysis of Codendronized Polymers. DSC traces of the codendronized polymers are shown in Figure 6. These polymers show endothermal peaks with peak temperatures at −20.8, −22.4, −15.3, and −16.3 °C, respectively. They are associated with melt of the crystallites of the long alkyl groups on the periphery of Percec-type dendrons. Clearly, the melting point increases with the dendron **2[G*n*]** generation. Different from the conventional linear polymer, like PS, PMMA, etc., the present codendronized polymers do not show a clear glass transition in the temperature range covered in this experiment. From Figure 6, we can see relatively broad transitions. The glass transition temperatures, T_g, of the four polymers are 56.0, 52.3, 59.2, and 56.1 °C, respectively. Clearly, the size increase of the two kinds of dendrons has different influences on T_g of the polymers. The flexible polyester-type dendron can soften the codendronized polymers, so their size increase causes a decrease of T_g. Yet relatively rigid Percec-type dendrons can harden the codendronized polymers, so large dendrons may increase T_g. Finally, like other Percec-type homo-dendronized polymers,[15] our codendronized polymers have a hexagonal columnar arrangement in melt (see SAXS data in the following subsection). In the temperature range covered in this experiment, there exist no obvious signals related to the first-order transition from hexagonal columnar phase to isotropic phase in DSC curves for these copolymers. Possibly, this result indicates that the hexagonal columnar phase of these polymers is relatively stable.

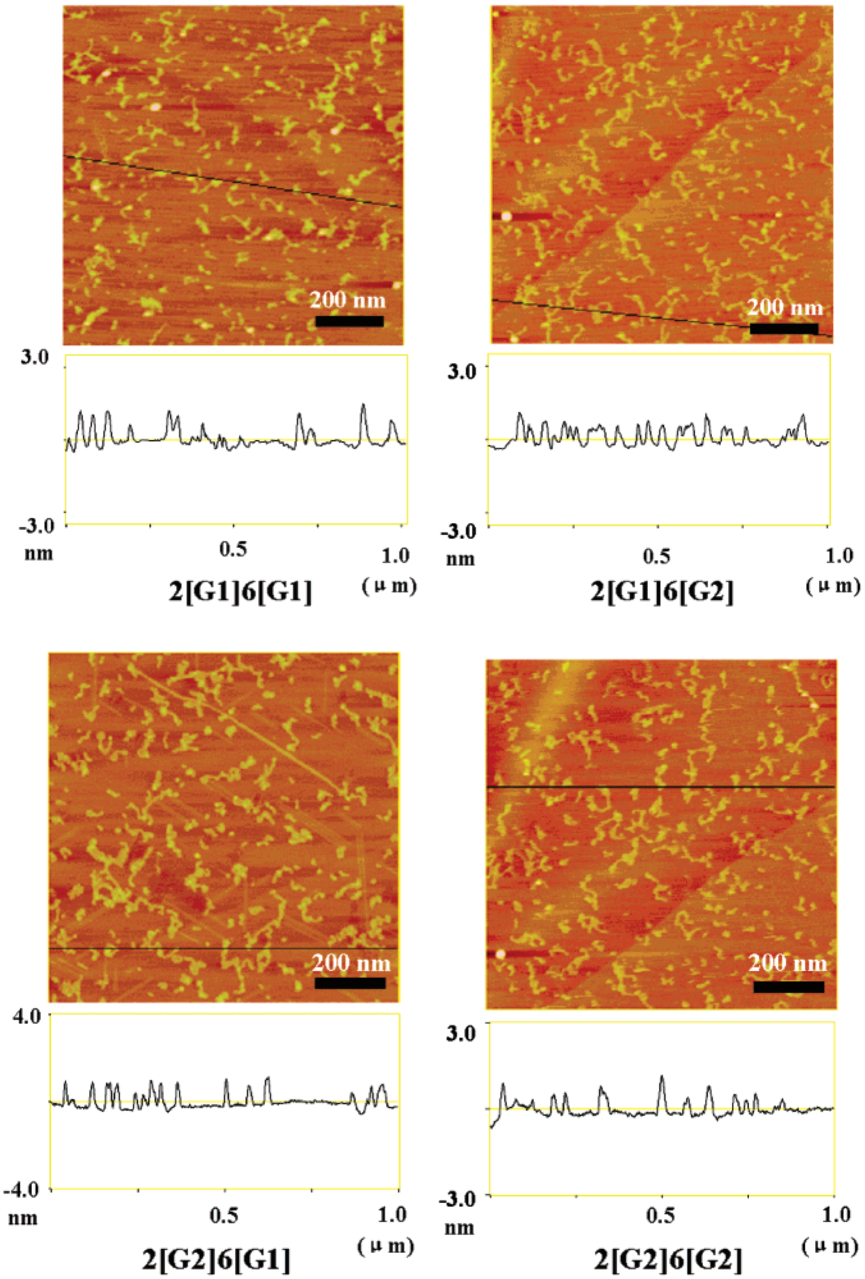

Figure 7. AFM micrographs of four codendronized polymers absorbed on HOPG.

AFM Analysis of Codendronized Polymers. Molecular morphologies of the codendronized polymers were studied using AFM analysis. The samples were prepared by spin-casting the dilute solutions (1×10^{-5} g/mL) onto a freshly cleaved highly oriented pyrolytic graphite (HOPG) at 1500 rpm. The AFM micrographs of four codendronized polymers are shown in Figure 7.

As demonstrated in these images, the molecular diameter seems not uniform from the image of **2[G1]6[G1]**, which might be due to intermolecular entanglement. Yet the rest of the polymers seem more uniform. It is noteworthy that the cylinders of **2[G2]6[G1]** and **2[G2]6[G2]** seem to adopt a meander-like conformation, which have been observed from the morphologies of poly(comacromonomers) brushes with linear branches.[16] The contour length of some molecules reached 100 nm. However, the distribution of the main chain length is broad due to the nature of conventional radical polymerization. From the cross-sectioned profiles in Figure 7, we may find that the monolayer height of every copolymer was uniform (about 1.2 ± 0.2 nm for **2[G1]6[G1]** and **2[G1]6[G2]**, about 2.0 ± 0.2 nm for **2[G2]6[G1]** and **2[G2]6[G2]**). The heights may have been underestimated due to the deformation of the samples on HOPG induced by the tapping tip.[17] Because the bulky dendrons are grafted alternately along the backbone, these polymers should hold a segmented structure, although direct visualization by AFM is not possible. It needs to be mentioned that these four codendronized polymers are not stiff enough to adopt a cylindrical morphology because of the low generation of dendritic wedges.

SAXS Analysis of the Bulk Materials of Codendronized Polymers. SAXS measurement was used to identify the supramolecular structures of these codendronized polymers in melt. The SAXS profiles of the four copolymers are shown in Figure 8.

Their scattering patterns show a strong scattering peak at lower *q* region and a weak shoulder at relatively higher *q* region

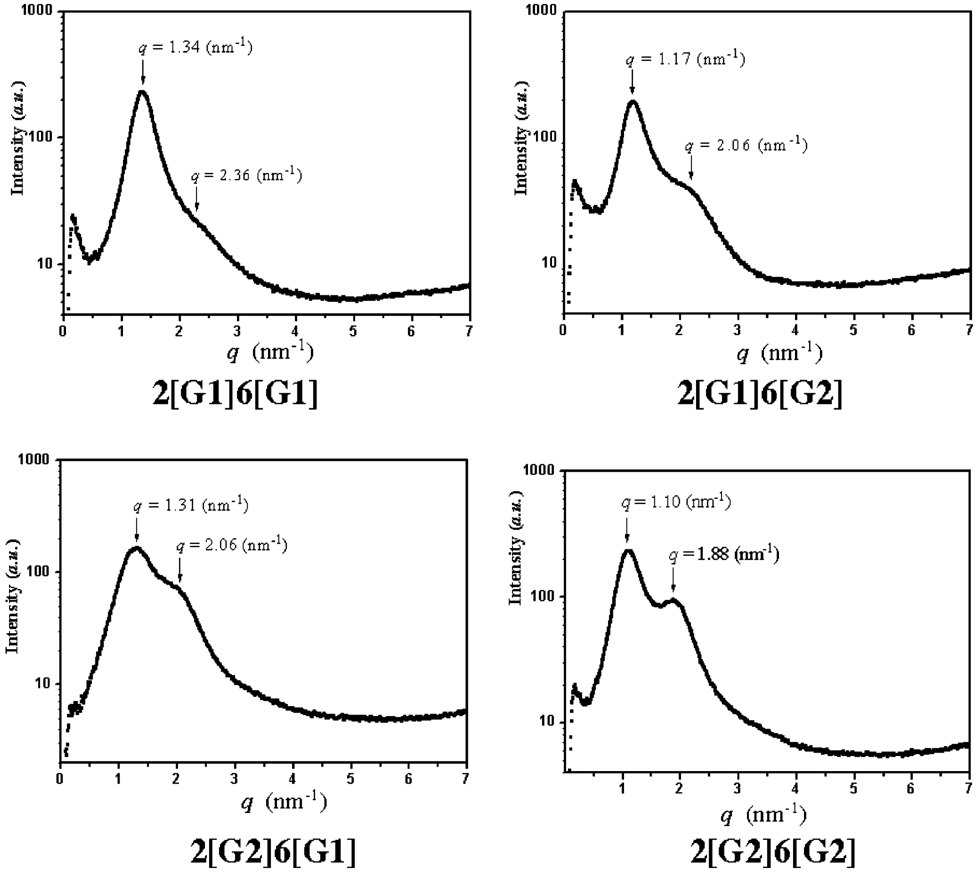

Figure 8. Small-angle X-ray scattering intensity profiles of the copolymers.

Scheme 4. Schematic Illustration of the Formation of Cylinder Structure of the 2[G*n*]6[G*n*] (*n* = 1, 2) Codendronized Polymer

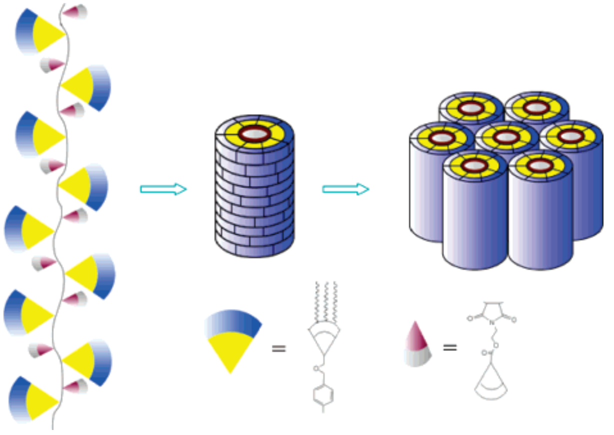

for the copolymers **2[G1]6[G1]**, **2[G1]6[G2]**, and **2[G2]6[G1]**, and two strong peaks for **2[G2]6[G2]**. The intensity of the scattering at the higher *q* region increases with the dendron generation. For **2[G2]6[G2]**, two separated scattering peaks indicate the formation of higher ordered structure. The ratios of the scattering peaks at lower and higher *q* regions are about $\sqrt{3}$, indicating the formation of hexagonally packed cylinders. However, the broad scattering peaks and the absence of higher order scattering peaks mean a lack of highly ordered structure. Because of the larger size and relatively rigidity of Percec-type polyether dendrons, the polyester dendrons may fill in the center of the cylinders, as shown in Scheme 4. In other words, the fan-shaped architecture of Percec-type polyether dendrons is the key factor of the formation of cylindrical structure of these codendronized polymers. Table 3 summarized the physical parameters of the cylindrical structure of these codendronized polymers evaluated from the SAXS data. Meanwhile, the diameter (*D*) of the supramolecular columns, the solid angle (α') of the dendrons, and the number of dendrons (μ) in the cross section of per column were calculated according to the reported methods,[18] and the results are also summarized in Table 3.

In Table 3, the cylinder diameters, *D*, are 5.37 nm for **2[G1]6[G1]**, 6.14 nm for **2[G1]6[G2]**, 5.82 nm for **2[G2]6[G1]**, and 6.64 nm for **2[G2]6[G2]**. Clearly, *D*-value increases with the dendron generation. More interesting is that the change caused by the polyester dendron from **6[G1]** to **6[G2]** is larger than that caused by Percec-type polyether dendron from **2[G1]** to **2[G2]**. As shown in Scheme 5, for example, when the center-located polyester dendrons are kept at the first generation, Percec-type dendron increases from the first generation in **2[G1]6[G1]** to the second generation in **2[G2]6[G1]**, the increment of cylinder diameter is about 0.45 nm, and, meanwhile, the dendron number, μ, per cross section decreases from 7 to 4, meaning that the sector was widened. However, when the centered volume was extended by increasing the polyester dendron from the first generation **6[G1]** to the second generation **6[G2]**, the increment of cylinder diameter is about 0.77 nm. The μ-value remains 7. In other words, 7 pieces of the first generation of Percec-type dendrons (**2[G1]**) construct the cylinders. This further means that the increasing size of polyester dendrons located in the center can result in a great change of the column diameter. Therefore, these codendronized polymers should adopt an interesting core–shell structure: two kinds of dendrons form a core that is composed of segmented Percec-type dendrons and polyester dendrons; long alkyl chains

Table 3. Structural Parameters of Columnar Structures of the Four Codendronized Polymers

monodendron	lattice	$\langle d_{100}\rangle^a$ (Å)	a^b (Å)	D^c (Å)	ρ^d (g/cm^3)	μ^e	α'^f (deg)
2[G1]6[G1]	*P*6*mm*	46.5	53.7	53.7	1.14	7	51.4
2[G1]6[G2]	*P*6*mm*	53.2	61.4	61.4	1.17	7	51.4
2[G2]6[G1]	*P*6*mm*	50.2	58.2	58.2	1.10	4	90.0
2[G2]6[G2]	*P*6*mm*	57.5	66.4	66.4	1.12	4	90.0

[a] $\langle d_{100}\rangle = (d_{100} + \sqrt{3}d_{110})/2$. [b] Hexagonal columnar lattice parameter $a = 2\langle d_{100}\rangle/\sqrt{3}$. [c] Columnar diameter $D = 2\langle d_{100}\rangle/\sqrt{3}$. [d] From calculation according to the literature.[19] [e] Number of dendrons per *p*6*mm* hexagonal column stratum $\mu = (\sqrt{3}N_AD^2t\rho)/2M$. [f] Projection of the solid angle for tapered and conical dendron $\alpha' = 2\pi/\mu$(deg). Avogadro's number $N_A = 6.0220455 \times 10^{23}$ mol^{-1}, the height of the column stratum was assumed as $t = 4.7$ Å, and M = molar mass of dendron.[18]

Scheme 5. Schematic Representation of the Changes of the Diameter (*D*) of the Supramolecular Columns and the Number of Dendrons (*μ*) in the Cross Section per Column for the Four Dendronized Copolymers

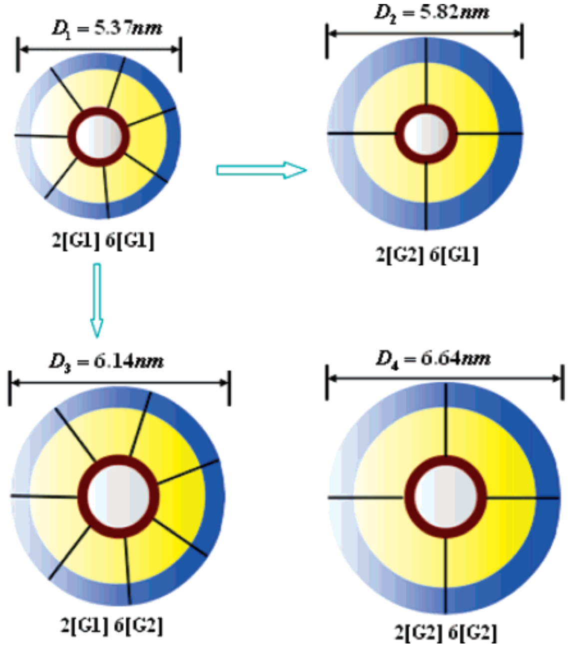

construct a shell to cover the core. Such core−shell cylinders packed into a hexagonal structure in the bulk. Therefore, the codendronized polymers with segmented structure organize hexagonally in bulk, and the novel materials with structures-in-structures are obtained.

Deprotection of Copolymers. The isopropylidene groups of −OH groups in four copolymers could be removed using Dowex H$^+$ resin in the mixture of THF and MeOH. The hydrolyzed products were confirmed by ^{13}C NMR and IR spectroscopy. No signals of carbons of protective groups at 23.7 ppm in the ^{13}C NMR spectrum were found, and, meanwhile, obvious absorption of −OH groups at 3450 cm^{-1} in IR spectrum was observed, indicating the protective groups were removed completely from the copolymers (see Figures S16 and S17 in the Supporting Information for the spectra of ^{13}C NMR and IR). The ^{1}H NMR spectra of them are shown in Figure S18 in the Supporting Information, further supporting the deprotection. Self-assembly and supramolecular properties of such amphiphilic wormlike dendronized polymers are currently studied.

Conclusion

We have studied the radical copolymerization of styryl polyether dendron and maleimide polyester dendron initiated by AIBN. The copolymers have been confirmed to hold a strict alternating sequence in microstructure by using ^{13}C NMR analysis. Because alternately grafted dendritic wedges are rather big relative to small organic groups, novel codendronized polymers may be considered as the linear polymers with segmented structure. Because the generations of each dendritic monomer are varied, the size of each segment is different, which may tune their structures. SAXS data indicate that these polymers with fine structure form cylinders in bulk state and the *D*-value increases with the pendent dendron generation. The present results demonstrate the molecular worms with segmented structure can be prepared by alternating radical copolymerization of dendritic monomers, which would be important to study the properties of well-defined molecules in nanometer scale.

Experimental Section

Materials. 4-Vinylbenzyl chloride (tech 90%, Acros), lithium tetrahydroaluminate ($LiAlH_4$; typically 97%, Alfa), sodium hydride (NaH; 60% dispersed in mineral oil, Aldrich), potassium iodide (KI; Beijing Chemicals Co.), and anhydrous potassium carbonate (K_2CO_3; AR, Beijing Chemicals Co.) were used as received. AIBN was recrystallized from ethanol. Maleic anhydride (MAn) was recrystallized from benzene. Other reagents were used without further purification. Dendritic alcohol **1[G1]-OH**,[20] protected *N*-hydroethyl maleimide **3b**,[21] *N*-hydroethyl maleimide,[22] and protected anhydride monomer **4**[23] were prepared (all of purity ≥98%) according to literature procedures.

General Procedures. Anhydrous dichloromethane (CH_2Cl_2) was distilled from CaH_2. Anhydrous ethyl ether (Et_2O), tetrahydrofuran (THF), and toluene were distilled from sodium. Thin-layer chromatography was performed using silica gel 60 F254 precoated plates (0.2 mm thickness). Column chromatography was carried out using 200−300 mesh silica gel.

Measurement. Common NMR spectra were acquired in $CDCl_3$ on a Bruker DMX-400 spectrometer at 400 MHz for ^{1}H NMR and 100 MHz for ^{13}C NMR, and the chemical shifts were given in δ values from TMS as an internal standard. Integrable quantitative carbon spectra were obtained by inverse gated-decoupling experiment in $CDCl_3$ on a Bruker DMX-600 spectrometer at 150 MHz. Polydispersities of polymers, M_w/M_n, were obtained by SEC equipped with a Waters 515 pump, a Waters 2414 refractive index detector, and a combination of column Styragel HT-2, HT-3, and HT-4; the effective molar mass ranges were 100−10 000, 500−30 000, and 5000−600 000, respectively. Linear polystyrene standards were applied as the calibration. The eluent was THF at a flow rate of 1.0 mL/min at 35 °C. The absolute molar masses of them were determined by GPC-TALLS equipping a Postnova pump (PN 1011), a mixed bead column (Polymer Laboratory Inc., 5 μm), and a PD2100 detector system (Precision Detector Inc., including a two-angle laser light scattering detector (TALLS) at 15° and 90°, a dynamics light scattering detector, and a differential refractive detector). The light source is a plane-polarized solid-state laser emitting at 809 nm. The GPC-TALLS characterization of the codendronized polymers was carried out with THF as eluent at a flow rate of 0.5 mL/min at 25 °C. The instrument was calibrated with narrow PS standard with number-average molecular weight of 25 000. The d*n*/d*c* values of codendronized polymers were obtained from this equipment and are listed in Table 2. MALDI-TOF (matrix-assisted laser desorption and ionization time-of-flight) mass spectrum was performed on a Bruker Biflex III spectrometer equipped with a 337 nm nitrogen laser. Both matrix 4-hydroxy-(*R*)-cyanocinnamic acid (CCA) and sample were dissolved in 1:1 (v/v) acetonitrile:water with 1% trifluoroacetic acid. 0.5 μL of this mixture solution was placed on a metal sample plate and air-dried at ambient temperature. Mass spectra were acquired in positive reflector mode using an acceleration voltage of 19 kV. External mass calibration was performed using a standard peptide mixture. Spectra were obtained by setting the laser power close to the threshold of ionization, and generally 100 pulses were acquired and averaged. FT-IR spectra were recorded by a deuterate triglycine sulfate (DTGS) detector on a Bruker EQUINOX 55 spectrometer and processed by the Bruker OPUS program. THF solution (20 mg/mL) was dropped on KBr flake and dried before tested. Thermal properties of the codendronized polymers were determined using a Diamond DSC system at scanning rates of ±10 °C/min under nitrogen atmosphere. AFM images were obtained under ambient conditions using a Digital Instrument Multimode Nanoscope IIIA operating in the tapping mode. Si cantilever tips (TESP) with a resonance frequency of approximately 300 kHz and a spring constant of about 40 N m^{-1} were used. The scan rate varied from 0.5 to 1.5 Hz. The set-point amplitude ratio was maintained at 0.9 to minimize the sample deformation induced by the tip. All AFM images were subjected to a first-order plane-fitting procedure to compensate for sample tilt. The samples for tapping mode AFM measurements were prepared by spin-casting the dilute solutions onto a freshly cleaved mica surface at 1500 rpm. SAXS experiments were recorded using a SAXS equipment with a two-dimensional detector (Brucker Histar), operated at 40 kV and 35 mA. The wavelength of the incident X-ray beam from Cu Kα radiation was $\lambda = 0.154$ nm. The distance between the sample and the detector was 27.4 cm. The long period was determined from the position of peak maxima in intensity curves (ln *I* vs *q*, where $q = 4\pi \sin \theta/\lambda$ and 2θ was the scattering angle). The *s*-axis was calibrated using several diffraction orders of silver behenate.

Synthesis and Polymerization. Synthesis of 2[G1, G2]. A detailed procedure can be found in the Supporting Information.

Synthesis of 5. The protected *N*-hydroethyl maleimide **3b** (0.5 g, 2.39 mmol) and DMAP (40 mg, 0.33 mmol) were dissolved in 20 mL of CH_2Cl_2, and 1 mL of pyridine was added. Anhydride **4** (1.58 g, 4.78 mmol) was added, and the reaction mixture was stirred at room temperature overnight. Stirring the reaction mixture with 5 mL of a pyridine:water (v:v, 1:1) solution overnight quenched the excess anhydride. The organic phase was diluted with 50 mL of CH_2Cl_2 and extracted with 1 M $NaHSO_4$ (3 × 30 mL), 10% Na_2CO_3 (3 × 30 mL), and saturated brine (30 mL). The organic phase was dried with $MgSO_4$, filtered, and the filtrate was evaporated to give 0.74 g (85%) of **5** as a light yellow liquid. ^{1}H NMR ($CDCl_3$) δ: 1.12 (s, H, C*H*$_3$), 1.30 (s, H, C*H*$_3$), 1.34 (s, H, C*H*$_3$), 2.80 (s, 2H,C*H*), 3.52 (d, $J = 11.67$ Hz, 2H, OC*H*$_2$), 3.71 (t, 2H, NC*H*$_2$), 4.07 (d, $J = 11.67$ Hz, 2H, OC*H*$_2$), 4.22 (t, 2H, COOC*H*$_2$), 5.19 (s, 2H, 2C*H*O), 6.44 (s, 2H, 2C*H*$_{vinyl}$). ^{13}C NMR ($CDCl_3$) δ: 18.52 (1C, *C*H$_3$), 23.36 (1C, *C*H$_3$), 23.99 (1C, *C*H$_3$), 37.82 (1C, *C*H$_3$), 41.73 (1C, *C*(CH$_3$)$_2$), 47.50 (2C, *C*H), 61.22 (1C, O*C*H$_2$), 65.81 (2C, 2*C*H$_2$), 80.87 (2C, *C*HO), 98.04 (1C, CH$_3$*C*CO), 136.34 (1C, *C*H$_{vinyl}$), 136.57 (1C, *C*H$_{vinyl}$), 173.98 (1C, *C*O$_{ester}$), 175.95 (2C, *C*O$_{imide}$). Mass spectrometry (MALDI-TOF) *m*/*z*: 404.1 $[M + K^+]^+$, 388.1 $[M + Na^+]^+$. Anal. Calcd for $C_{18}H_{23}NO_7$: C, 59.17; H, 6.34; N, 3.83. Found: C, 59.17; H, 6.38; N, 3.82.

Synthesis of Monomer 6[G1]. The product **5** (1.0 g, 2.40 mmol) was suspended in toluene (20 mL), and the mixture was heated to reflux. The reaction was monitored by TLC (SiO_2, EtOAc/PE = 1/1 (v/v), $R_{f(\mathbf{5})}$ 0.40, $R_{f(\mathbf{6[G1]})}$ 0.65). After 12 h, the solvent was removed under reduced pressure to give **6[G1]** (0.79 g, 95% yield) as a light yellow liquid. ^{1}H NMR ($CDCl_3$) δ: 1.10 (s, H, C*H*$_3$), 1.30 (s, H, C*H*$_3$), 1.34 (s, H, C*H*$_3$), 3.52 (d, $J = 11.67$ Hz, 2H, OC*H*$_2$C and OC*H*$_2$C), 3.76 (t, 2H, $J = 5.05$ Hz, NC*H*$_2$), 4.05 (d, $J = 11.67$ Hz, 2H, OC*H*$_2$C and OC*H*$_2$C), 4.24 (t, $J = 4.97$ Hz, 2H, OC*H*$_2$), 6.66 (s, 2H, 2C*H*$_{vinyl}$). ^{13}C NMR ($CDCl_3$) δ: 18.55 (1C, *C*H$_3$), 23.06 (1C, *C*H$_3$), 24.21 (1C, *C*H$_3$), 36.83 (1 C, *C*H$_3$), 41.77 (1C, *C* (CH$_3$)$_2$), 61.87 (1C, O*C*H$_2$), 65.81 (2C, 2*C*H$_2$), 98.08 (1C, CH$_3$*C*CO), 134.22 (2C, *C*H$_{vinyl}$), 170.32 (1C, *C*O$_{ester}$), 173.98 (2C, *C*O$_{imide}$). Mass spectrometry (EI-MS) *m*/*z*: 298 $[M + H^+]^+$. Anal. Calcd for $C_{14}H_{19}NO_6$: C, 56.56; H, 6.44; N, 4.71. Found: C, 56.81; H, 6.47; N, 4.85.

Synthesis of Diol 7. Compound **5** (1.00 g, 2.40 mmol) was dissolved in 50 mL of methanol. Three teaspoons of Dowex H$^+$ resin was added, and the reaction mixture was stirred for 3 h at room temperature. When the reaction was complete, the Dowex H$^+$ resin was filtered off in a glass filter and carefully washed with methanol. The methanol was evaporated to give **7** as light yellow liquid in the yield of 95%. ^{1}H NMR ($CDCl_3$) δ: 1.01 (s, H, C*H*$_3$), 2.87 (s, 2H, 2C*H*), 3.20−3.10 (2H, 2O*H*), 3.63 (d, $J = 11.37$ Hz, 2H, CC*H*$_2$), 3.77−3.71 (m, 4H, NC*H*$_2$, CC*H*$_2$), 4.27 (t, 2H, COOC*H*$_2$), 5.24 (s, 2H, 2C*H*O), 6.49 (s, 2H, 2C*H*$_{vinyl}$). ^{13}C NMR ($CDCl_3$) δ: 17.10 (1C, *C*H$_3$), 37.95 (1C, N*C*H$_2$), 47.47 (2C, 2*C*H), 49.60 (1C, CO*C*), 61.39 (1C, O*C*H$_2$), 67.10 (2C, 2*C*H$_2$OH), 80.89 (2C, 2*C*HO), 136.46 (2C, *C*H$_{vinyl}$), 175.35 (1C, *C*O$_{ester}$), 176.44 (2C, *C*O$_{imide}$). Mass spectrometry (EI-MS) *m*/*z*: 326 $[M + H^+]^+$. Anal. Calcd for $C_{15}H_{19}NO_7$: C, 55.38; H, 5.89; N, 4.31. Found: C, 54.42; H, 5.89; N, 4.12.

Synthesis of 8. Compound **7** (0.19 g, 0.58 mmol) and DMAP (6.2 mg, 0.051 mmol) were dissolved in 10 mL of CH_2Cl_2, and 1 mL of pyridine was added. Anhydride **4** (0.5 g, 1.53 mmol) was added, and the reaction mixture was stirred at room temperature overnight. Stirring the reaction mixture with 5 mL of a 1:1 pyridine: water solution quenched the excess anhydride overnight. The organic phase was diluted with 50 mL of CH_2Cl_2 and extracted with 1 M $NaHSO_4$ (3 × 30 mL), 10% Na_2CO_3 (3 × 30 mL), and saturated brine (30 mL). The organic phase was dried with $MgSO_4$, filtered, and the filtrate evaporated to give 0.23 g (60%) of **8** as a light yellow liquid. ^{1}H NMR ($CDCl_3$) δ: 1.14 (s, 6H, 2C*H*$_3$), 1.26 (s, 3H, C*H*$_3$), 1.34 (s, 6H, 2C*H*$_3$), 1.40 (s, 6H, 2C*H*$_3$), 2.90 (s, 2H, 2C*H*), 3.61 (d, $J = 11.64$ Hz, 4H, 2OC*H*$_2$), 3.77 (t, $J = 4.84$ Hz, 2H, NC*H*$_2$), 4.13 (d, $J = 11.68$ Hz, 4H, 2OC*H*$_2$), 4.31−4.22 (m, 6H, COOC*H*$_2$ and 2OC*H*$_2$C), 5.29 (s, 2H, 2C*H*O), 6.51 (s, 2H, 2C*H*$_{vinyl}$). ^{13}C NMR ($CDCl_3$) δ: 17.43 (1C, *C*H$_3$), 18.55 (2C, 2*C*H$_3$), 22.32 (2C, 2*C*H$_3$), 24.92 (1C, 2*C*H$_3$), 37.63 (1C, N*C*H$_2$), 42.01 (1C, *C*(CH$_3$)$_2$), 46.74 (1C, *C*H), 47.58 (1C, *C*H), 61.76 (1C, O*C*H$_2$), 65.18 (2C, 2O*C*H$_2$), 65.94 (4C, 4O*C*H$_2$), 80.87 (2C, *C*HO), 98.09 (3C, 3CH$_3$*C*CO), 136.55 (2C, *C*H$_{vinyl}$), 172.19 (1C, *C*O$_{ester}$), 173.53 (2C, 2*C*O$_{ester}$), 176.11 (2C, *C*O$_{imide}$). Mass spectrometry (MALDI-TOF) *m*/*z*: 660.2 $[M + Na^+]^+$.

Synthesis of Monomer 6[G2]. Compound **8** (0.2 g, 0.31 mmol) was suspended in toluene (20 mL), and the mixture was heated to reflux. The reaction was monitored by TLC (SiO_2, EtOAc/PE = 1/1, $R_{f(\mathbf{8})}$ 0.34, $R_{f(\mathbf{6[G2]})}$ 0.56). After 12 h, the solvent was removed under reduced pressure to give **6[G2]** (0.17 g, 95% yield) as a light yellow liquid. ^{1}H NMR ($CDCl_3$) δ: 1.14 (s, 6H, 2C*H*$_3$), 1.25 (s, 3H, C*H*$_3$), 1.34 (s, 6H, 2C*H*$_3$), 1.40 (s, 6H, 2C*H*$_3$), 3.60 (d, $J = 11.64$ Hz, 4H, 2OC*H*$_2$), 3.80 (t, $J = 5.08$ Hz, 2H, NC*H*$_2$), 4.13 (d, $J = 11.72$ Hz, 4H, 2OC*H*$_2$), 4.30−4.23 (m, 6H, COOC*H*$_2$ and 2OC*H*$_2$C), 6.73 (s, 2H, 2C*H*$_{vinyl}$). ^{13}C NMR ($CDCl_3$) δ: 17.51 (1C, *C*H$_3$), 18.54 (2C, 2*C*H$_3$), 22.28 (2C, 2*C*H$_3$), 24.93 (1C, 2*C*H$_3$), 36.73 (1C, N*C*H$_2$), 42.02 (1C, *C* (CH$_3$)$_2$), 46.74 (1C, *C*(CH$_3$)$_2$), 62.48 (1C, O*C*H$_2$), 65.19 (1C, O*C*H$_2$C), 65.93 (2C, 2O*C*H$_2$C), 65.95 (3C, 3O*C*H$_2$C), 98.10 (3C, 3CH$_3$*C*CO), 134.25 (2C, 2*C*H$_{vinyl}$), 170.32 (1C, *C*O$_{ester}$), 172.29 (2C, 2*C*O$_{ester}$), 173.49 (2C, *C*O$_{imide}$). Mass spectrometry (MALDI-TOF) *m*/*z*: 592.1 $[M + Na^+]^+$, 608.1 $[M + K^+]^+$. Anal. Calcd for $C_{27}H_{39}NO_{12}$: C, 56.93; H, 6.90; N, 2.46. Found: C, 56.80; H, 6.84; N, 2.57.

General Procedure for Copolymerization of Monomers: Synthesis of Their Copolymers. 2[Gn], **6[Gn]** ($n = 1, 2$), AIBN, and dry chloroform were placed in a Schlenk flask with a magnetic stir bar and a rubber septum. The polymerization mixture was degassed with a freeze−evacuate−thaw cycle three times and sealed. The reaction was carried out at 60 °C in an oil bath, until the magnetic stir bar could not move, usually in 2−5 h. The polymer was dissolved in chloroform and precipitated in MeOH until no monomer remained as analyzed by SEC and ^{1}H NMR. See the Supporting Information for details.

General Procedure for Hydrolysis of the Copolymers. The copolymer was dissolved in the mixture of THF and MeOH (3/1, v/v, 30 mL) at room temperature to give the solutions of concentration of 50 mg/mL. Three teaspoons of Dowex H$^+$ resin was added, and the reaction mixture was stirred for 3 h at room temperature. When the reaction was complete, the Dowex H$^+$ resin was filtered off in a glass filter and carefully washed with THF. The liquid was evaporated at 30 °C. The residue was dissolved in THF and precipitated in MeOH. Finally, the amphiphilic copolymer was synthesized. Yet it was very unstable in the solid state because there were a lot of hydrogen bonds in the system.

Acknowledgment. Financial support by the National Science Foundation of China (20534010, 20374030, and 20625412) is greatly acknowledged. The Nankai group is thankful for financial support provided by the State Key Laboratory of Polymer Physics and Chemistry.

Supporting Information Available: Revised route to synthesize **1[G2]-OH**, synthesis of **2[G*n*]** ($n = 1, 2$) monomers, Figures S1–S18 of the ^{1}H NMR, ^{13}C NMR, mass spectra of monomer **2[G*n*]** ($n = 1, 2$), ^{1}H NMR spectra of copolymers **2[G1]6[G2]**, **2[G2]6-[G1]**, and **2[G2]6[G2]**, and ^{1}H NMR spectra of deprotected copolymers **D2[G1]6[G1]**, **D2[G1]6[G2]**, **D2[G2]6[G1]**, and **D2-[G2]6[G2]**. This material is available free of charge via the Internet at http://pubs.acs.org.

References and Notes

(1) (a) Fréchet, J. M. J.; Tomalia, D. A. *Dendrimers and Other Dendritic Polymers*; Wiley: New York, 2002. (b) Newkome, G. R.; Moorefield, C. N.; Vögtle, F. *Dendrimers and Dendrons, Concepts, Syntheses, Applications*; Wiley-VCH: Weinheim, 2001. (c) Chow, H.-F.; Mong, T. K.-K.; Nongrum, M. F.; Wan, C.-W. *Tetrahedron* **1998**, *54*, 8543–8660. (d) Matthews, O. A.; Shipway, A. N.; Stoddart, J. F. *Prog. Polym. Sci.* **1998**, *23*, 1–56. (e) Bosman, A. W.; Janssen, H. M.; Meijer, E. W. *Chem. Rev.* **1999**, *99*, 1665–1688. (f) Vögtle, F.; Gestermann, S.; Hesse, R.; Schwierz, H.; Windisch, B. *Prog. Polym. Sci.* **2000**, *25*, 987–1041.

(2) (a) Lo, S.-C.; Burn, P. L. *Chem. Rev.* **2007**, *107*, 1097–1116. (b) Tomalia, D. A.; Naylor, A. M.; Goddard, W. A. *Angew. Chem., Int. Ed. Engl.* **1990**, *29*, 138–175. (c) Tomalia, D. A.; Durst, H. D. *Top. Curr. Chem.* **1993**, *165*, 193–313. (d) Adronov, A.; Fréchet, J. M. J. *Chem. Commun.* **2000**, 1701–1710.

(3) (a) Schlüter, A. D.; Rabe, J. P. *Angew. Chem., Int. Ed.* **2000**, *39*, 864–883. (b) Stocker, W.; Schürmann, B. L.; Rabe, J. P.; Förster, S.; Lindner, P.; Neubert, I.; Schlüter, A. D. *Adv. Mater.* **1998**, *10*, 793–797. (c) Zhang, A. F.; Shu, L. J.; Bo, Z. S.; Schlüter, A. D. *Macromol. Chem. Phys.* **2003**, *204*, 328–339. (d) Frey, H. *Angew. Chem., Int. Ed.* **1998**, *37*, 2193–2197. (e) Percec, V.; Ahn, C.-H.; Ungar, G.; Yeardley, D. J. P.; Möller, M.; Sheiko, S. S. *Nature* **1998**, *391*, 161–164. (f) Malenfant, P. R. L.; Fréchet, J. M. J. *Macromolecules* **2000**, *33*, 3634–3640. (g) Percec, V.; Ahn, C. H.; Barboiu, B. *J. Am. Chem. Soc.* **1997**, *119*, 12978–12979. (h) Bo, Z. S.; Schlüter, A. D. *Chem.-Eur. J.* **2000**, *6*, 3235–3241.

(4) (a) Sheiko, S. S.; Möller, M. *Chem. Rev.* **2001**, *101*, 4099–4124. (b) Barner, J.; Mallwitz, F.; Shu, L. J.; Schlüter, A. D.; Rabe, J. P. *Angew. Chem., Int. Ed.* **2003**, *42*, 1932–1935. (c) Ecker, C.; Severin, N.; Shu, L. J.; Schlüter, A. D.; Rabe, J. P. *Macromolecules* **2004**, *37*, 2484–2489.

(5) (a) Lee, C. C.; Yoshida, M.; Fréchet, J. M. J.; Dy, E. E.; Szoka, F. C. *Bioconjugate Chem.* **2005**, *16*, 535–541. (b) Gillies, E. R.; Fréchet, J. M. J. *Drug Discovery Today* **2005**, *10*, 35–43. (c) Liang, C. O.; Helms, B.; Hawker, C. J.; Fréchet, J. M. J. *Chem. Commun.* **2003**, *20*, 2524–2525. (d) Fu, Y. Q.; Li, Y.; Li, J.; Yan, S.; Bo, Z. S. *Macromolecules* **2004**, *37*, 6395–6400.

(6) Marsitzky, D.; Vestberg, R.; Blainey, P.; Tang, B. T.; Hawker, C. J.; Carter, K. R. *J. Am. Chem. Soc.* **2001**, *123*, 6965–6972.

(7) (a) Karakaya, B.; Claussen, W.; Gessler, K.; Saenger, W.; Schlüter, A. D. *J. Am. Chem. Soc.* **1997**, *119*, 3296–3301. (b) Desai, A.; Atkinson, N.; JR, F. R.; Devonport, W.; Rees, I.; Branz, S. E.; Hawker, C. J. *J. Polym. Sci., Part A: Polym. Chem.* **2000**, *38*, 1033–1044. (c) Helms, B.; Mynar, J. L.; Hawker, C. J.; Fréchet, J. M. J. *J. Am. Chem. Soc.* **2004**, *126*, 15020–15021.

(8) (a) Yin, R.; Zhu, Y.; Tomalia, D. A.; Ibuki, H. *J. Am. Chem. Soc.* **1998**, *120*, 2678–2679. (b) Shu, L. J.; Schlüter, A. D.; Ecker, C.; Severin, N.; Rabe, J. P. *Angew. Chem., Int. Ed.* **2001**, *40*, 4666–4669.

(9) (a) Bo, Z. S.; Rabe, J. P.; Schlüter, A. D. *Angew. Chem., Int. Ed.* **1999**, *38*, 2370–2372. (b) Bo, Z. S.; Zhang, C. M.; Severin, N.; Rabe, J. P.; Schlüter, A. D. *Macromolecules* **2000**, *33*, 2688–2694. (c) Wu, C.-W.; Tsai, C.-M.; Lin, H.-C. *Macromolecules* **2006**, *39*, 4298–4305. (d) Zhu, B.; Han, Y.; Sun, M.; Bo, Z. S. *Macromolecules* **2007**, *40*, 4494–4500.

(10) (a) Zhang, A. F.; Barner, J.; Goessl, I.; Rabe, J. P.; Schlüter, A. D. *Angew. Chem., Int. Ed.* **2004**, *43*, 5185–5188. (b) Zhang, A. F.; Okrasa, L.; Pakula, T.; Schlüter, A. D. *J. Am. Chem. Soc.* **2004**, *126*, 6658–6666.

(11) Zhang, Y. H.; Huang, J.; Chen, Y. M. *Macromolecules* **2005**, *38*, 5069–5077.

(12) Zhang, Y. H.; Li, X. K.; Deng, G. H.; Chen, Y. M. *Macromol. Chem. Phys.* **2006**, *207*, 1394–1403.

(13) Zhang, Y. H.; Xu, Z. Z.; Li, X. K.; Chen, Y. M. *J. Polym. Sci., Part A: Polym. Chem.* **2007**, *45*, 3994–4001.

(14) Ha, N. T. H. *Polymer* **1999**, *40*, 1081–1086.

(15) Percec, V.; Ahn, C.-H.; Cho, W.-D.; Jamieson, A. M.; Kim, J.; Leman, T.; Schmidt, M.; Gerle, M.; Moller, M.; Prokhorova, S. A.; Sheiko, S. S.; Cheng, S. Z. D.; Zhang, A.; Ungar, G.; Yeardley, D. J. P. *J. Am. Chem. Soc.* **1998**, *120*, 8619–8631.

(16) (a) Stephan, T.; Muth, S.; Schmidt, M. *Macromolecules* **2002**, *35*, 9857–9860. (b) Gallyamov, M. O.; Tartsch, B.; Khokhlov, A. R.; Sheiko, S. S.; Börner, H. G.; Matyjaszewski, K.; Möller, M. *Chem.-Eur. J.* **2004**, *10*, 4599–4605.

(17) Winkler, R. G.; Spatz, J. P.; Sheiko, S. S.; Möller, M.; Reineker, P.; Marti, O. *Phys. Rev. B* **1996**, *54*, 8908–8912.

(18) (a) Percec, V.; Peterca, M.; Sienkowska, M. J.; Ilies, M. A.; Aqad, E.; Smidrkal, J.; Heiney, P. A. *J. Am. Chem. Soc.* **2006**, *128*, 3324–3334. (b) Percec, V.; Cho, W.-D.; Ungar, G. *J. Am. Chem. Soc.* **2000**, *122*, 10273–10281. (c) Zhu, X. M.; Scherbina, M. A.; Bakirov, A. V.; Gorzolnik, B.; Chvalun, S. N.; Beginn, U.; Möller, M. *Chem. Mater.* **2006**, *18*, 4667- 4673.

(19) (a) Immirzi, A.; Perini, B. *Acta Crystallogr.* **1977**, *A33*, 216–218. (b) Gao, Y.; Zhang, X. W.; Yang, M.; Zhang, X. J.; Wang, W.; Wegner, G.; Burger, C. *Macromolecules* **2007**, *40*, 2606–2612. (c) Pötschke, D.; Ballauff, M.; Lindner, P.; Fischer, M.; Vögtle, F. *Macromolecules* **1999**, *32*, 4079- 4087. (d) Ballauff, M. *Top. Curr. Chem.* **2001**, *212*, 177–194.

(20) Balagurusamy, V. S. K.; Ungar, G.; Percec, V.; Johansson, G. *J. Am. Chem. Soc.* **1997**, *119*, 1539–1555.

(21) Mantovani, G.; Lecolley, F.; Tao, L.; Haddleton, D. M.; Clerx, J.; Cornelissen, J. J. L. M.; Velonia, K. *J. Am. Chem. Soc.* **2005**, *127*, 2966–2973.

(22) Zentz, F.; Valla, A.; Guillou, R. L.; Labia, R.; Mathot, A. G.; Sirot, D. *IL Farmaco*. **2002**, *57*, 421–426.

(23) Gillies, E. R.; Fréchet, J. M. J. *J. Am. Chem. Soc.* **2002**, *124*, 14137–14146.

MA071507Y